

How Can Incentives and Cut Layer Selection Influence Data Contribution in Split Federated Learning?

Joohyung Lee, *Senior Member, IEEE*, Jungchan Cho, Wonjun Lee, *Fellow, IEEE*,
Mohamed Seif, and H. Vincent Poor, *Life Fellow, IEEE*

Abstract—To alleviate the training burden in federated learning while enhancing convergence speed, Split Federated Learning (SFL) has emerged as a promising approach by combining the advantages of federated and split learning. However, recent studies have largely overlooked competitive situations. In this framework, the SFL model owner can choose the cut layer to balance the training load between the server and clients, ensuring the necessary level of privacy for the clients. Additionally, the SFL model owner sets incentives to encourage client participation in the SFL process. The optimization strategies employed by the SFL model owner influence clients' decisions regarding the amount of data they contribute, taking into account the shared incentives over clients and anticipated energy consumption during SFL. To address this framework, we model the problem using a hierarchical decision-making approach, formulated as a single-leader multi-follower Stackelberg game. We demonstrate the existence and uniqueness of the Nash equilibrium among clients and analyze the Stackelberg equilibrium by examining the leader's game. Furthermore, we discuss privacy concerns related to differential privacy and the criteria for selecting the minimum required cut layer. Our findings show that the Stackelberg equilibrium solution maximizes the utility for both the clients and the SFL model owner.

Index Terms—Split Federated Learning, Wireless Networking, Game Theory, Incentive Mechanism, Cut Layer Selection.

I. INTRODUCTION

Recent innovations in Distributed Collaborative Machine Learning (DCML) have opened new possibilities for developing scalable and accurate Artificial Intelligence (AI) solutions. By leveraging diverse datasets across multiple clients without transmitting personal data to a central server, these methods significantly reduce the risk of privacy leakage. Federated learning (FL) and split learning (SL) are two popular approaches, though both face practical limitations [1]–[3]:

- FL: FL allows a server model to be trained in parallel across many clients, but each client is required to run an entire model, resulting in a significant training burden. This leads to high battery consumption on clients, significant client-side computation requirements, and limited model privacy.
- SL: SL splits the entire model into smaller portions, allowing only a shallow sub-network to be trained on the

client side, thus reducing the training burden. However, the training process is sequential, and client models are not aggregated, leading to significant time overhead.

To overcome these limitations, a new distributed learning framework, Split Federated Learning (SFL), has recently been proposed. SFL combines the advantages of both FL and SL, aiming to reduce the training burden of FL while enhancing convergence speed. More specifically, in SFL, clients train only a portion of the entire model, known as the client-side model, which decreases their computational load. These client-side models are then synchronized to enhance convergence speed via FL process [2], [4].

However, despite its notable advantages, SFL introduces additional communication overhead when interacting with servers and also raises privacy concerns due to the frequent exchange of client-side model outputs and updates, which are correlated to raw data. Optimizing SFL management to address these challenges remains a complex issue [1], [2]. Hence, there have been various approaches to managing SFL in the literature, aiming to achieve efficient communication in SFL operations. These approaches consider factors such as cut layer selection, clustering, management of radio and computational resources (e.g., CPU/GPU), and gradient compression [2], [5]–[8].

Nevertheless, the aforementioned work assumes that clients are motivated to voluntarily participate in the SFL process without any incentives. In reality, participating in the SFL process requires substantial energy consumption, which depends on the complexity of the client-side model and the amount of data contribution to train the model from the client's perspective. Therefore, without suitable incentives that take into account the cut layer selection (i.e., the complexity of the client-side model), motivating clients to engage in the SFL process to generate an accurate model is challenging. Although there have been various studies on incentive mechanisms in FL (see, for example, [9] and the references therein), there exist no studies specifically addressing SFL's unique characteristics as follows. i) Competition arises between the SFL model owner, who aims to create a global model from the SFL process for AI services, and the clients, who participate in the SFL process. Additionally, given the incentives, there is further competition among clients striving to earn more rewards. Thus, understanding the clients' reactions to the optimal decisions and behaviors of the SFL model owner is crucial. ii) This necessitates a careful study of sophisticated incentive mechanisms and cut layer selection, considering how these competitive behaviors can influence the data contributions of clients. For instance, if the client-side model size increases,

J. Lee and J. Cho are with the School of Computing, Gachon University, Seongnam 13120, Rep. of Korea (e-mail: j17.lee@gachon.ac.kr; thinkai@gachon.ac.kr).

W. Lee is with the School of Cybersecurity, Korea University, Seoul, Rep. of Korea (e-mail: wlee@korea.ac.kr).

M. Seif and H. V. Poor are with the Department of Electrical and Computer Engineering, Princeton University, Princeton, NJ 08544 USA (e-mail: mseif@princeton.edu; poor@princeton.edu).

Corresponding author: Jungchan Cho.

resulting in higher model complexity, clients will face a greater training burden. This may lead them to reduce their data contributions unless they receive sufficient incentives.

To the best of our knowledge, our work is the first to examine the competitive situation between clients and the SFL model owner during the SFL process. Our aim is to design an integrated approach to cut layer selection and incentive management from the SFL model owner's perspective, as well as data contribution management from the clients' perspective. Our contributions are summarized as follows:

- We investigate the interactions between the SFL model owner and clients, which create competitive situations during the SFL process. This is formulated as a single-leader and multi-follower game.
- To achieve this, we develop analytical models to explore the trade-offs for the SFL model owner, including satisfaction with the acquired training data, load reduction, and payment for incentives. For the clients, we examine the balance between the energy consumption required for the SFL process and the anticipated incentives.
- We derive closed-form expressions for the Nash equilibrium among heterogeneous clients and develop algorithms to obtain Stackelberg strategies by proving the existence of these solutions. Additionally, we discuss privacy enhancements related to cut layer selection and differential privacy.
- Our findings show that the Nash and Stackelberg strategies are desirable operating points for all participants (i.e., the SFL model owner and clients) in competitive situations. From our classification experiments using the CIFAR-10 dataset, we highlight the importance of incentive mechanisms in accelerating SFL and enhancing model accuracy. In our experiment, accuracy varies from 60% to 91% depending on the incentives provided. Specifically, we evaluate the effectiveness of these strategies under various parameter settings, which motivates the design of incentive mechanisms for practical SFL applications.

The remainder of this paper is organized as follows. Section II reviews related work on cut layer selection and resource management for SFL. Section III presents the system model and formulates the utility functions for both the SFL model owner and the clients. In Section IV, we describe the competitive game between the SFL model owner and the clients, rigorously formulating the problem as a Stackelberg game. We then characterize the closed-form solutions for a Nash Equilibrium of the clients and provide the algorithm to obtain a Stackelberg Equilibrium. Section V provides the performance evaluation. Section VI discusses the impact of cut layer selection and differential privacy on the privacy level, offering guidelines for setting the minimum cut layer requirements during the SFL process. Finally, Section VII concludes the paper and suggests directions for future research.

II. RELATED WORK

To mitigate the training burden in FL and improve convergence speed, SFL has emerged as a promising method, integrating the benefits of federated and split learning. However,

SFL is associated with substantial communication overhead, mainly due to the transfer of smashed data, gradients, and model updates between clients, the main server, and the federated server. This necessitates enhancements [7]. Recent studies have focused on the impact of cut layer selection on system performance and privacy. Notably, [2], [5] developed analytical models to explore the effect of total model training time (latency) on the cut layer point. Based on these analyses, various strategies have been proposed to enhance communication efficiency in SFL [5]–[7]. For instance, [5] introduced an optimal cut layer selection method based on latency analysis, followed by a convergence analysis of the SFL framework. Extending this work, [6] examined the latency of SFL in wireless networks and designed a joint optimization problem involving cut layer selection, client clustering, and bandwidth allocation to minimize overall training latency. Similarly, [10] proposed a joint method for cut layer selection and server computation resource allocation for clients. [7] employed an auxiliary network for local updates of client-side models, maintaining only a single server-side model to reduce storage costs on the main server, and conducted a comprehensive analysis of communication costs, storage space, and convergence. Additionally, [8] focused on reducing the dimensions of activations' gradients for backpropagation to decrease communication overhead. This study also explored joint optimization strategies for subchannel allocation, power control, and cut layer selection in wireless networks, aiming to minimize per-round latency. The recent work of [11] utilized SFL for Unmanned Aerial Vehicles (UAVs) networks considering wireless network perspectives. It generated the mobile traffic prediction model from UAVs collaboratively by selecting the cut layer in SFL for energy-efficient training.

In addition to these efficiency considerations, SFL poses privacy concerns due to interactions between clients and servers, including both the main and federated servers. During the forward phase, clients transmit smashed data to the main server, which becomes vulnerable to reconstruction attacks, potentially compromising the privacy of the original information. Furthermore, exchanging model updates with the federated server introduces additional risks to raw data privacy. To address these issues, several privacy-preserving mechanisms have been proposed. For instance, a recent study [12] on split learning empirically investigated the impact of cut layer selection on reconstruction attacks during the forward phase. The findings suggested that having deeper layers on the client side, which involve more non-linear functions, compresses raw data by eliminating less informative features, thereby enhancing resistance to reconstruction attacks. Similarly, [13] conducted empirical studies on how the distance correlation between raw and smashed data affects privacy leakage in split learning, emphasizing the importance of cut layer selection. Recently, the work in [14] analyzed the trade-off between energy consumption and privacy levels in relation to cut-layer selection in SFL. Furthermore, the work of [15] introduced an innovative cut layer selection scheme aimed at reducing the overall training latency in SFL, taking into account wireless network perspectives. Specifically, the proposed scheme not only minimized the overall training latency but also ensured

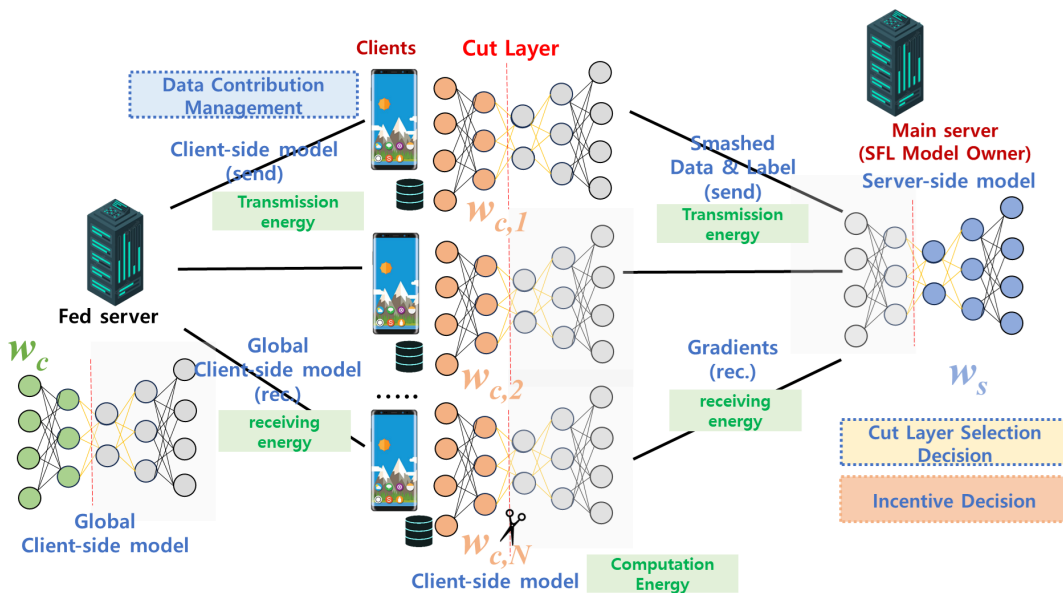


Fig. 1: Concept of the proposed Split Federated Learning: It considers interactions between the model owner and clients. The SFL model owner determines the cut layer and incentives, while the clients manage data contribution, considering their energy consumption.

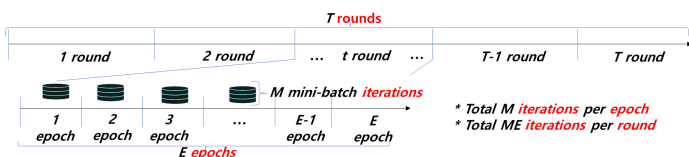


Fig. 2: Timeline of the Overall SFL Process.

an acceptable level of privacy by setting boundary constraints on the cut layer selection.

However, none of these studies address the strategic mechanisms of the SFL model owner and clients considering their competitive behaviors, which is one of our contributions. Notably, our approach to formulating and analyzing a Stackelberg game with two solution concepts involving the SFL model owner and clients is not fully covered in previous work.

III. SYSTEM MODEL

The SFL framework consists of two servers (which can be either physical or logical servers): (i) a federated learning server, referred to as the fed server, and (ii) a main server, along with multiple clients participating as part of the SFL process. In this setup, we define a set of clients as $\mathcal{N} = 1, 2, \dots, N$, where each client is represented as $n \in \mathcal{N}$ and has its own local dataset \mathcal{D}_n . The size of each dataset \mathcal{D}_n is indicated by the number of data items, denoted as $D_n = |\mathcal{D}_n|$, with each data item comprising both features and labels. The entire model, denoted as w , is composed of L layers. Specifically, the model w is divided into two sub-models at the L_c -th layer, referred to as the cut layer. These sub-models are: (i) the client-side model w_c , including layers from the first layer up to layer L_c , and (ii) the server-side model w_s , encompassing layers from layer $L_c + 1$ to layer L .

Thus, the full model can be represented as $w = [w_c; w_s]$. As shown in Fig. 1, each client n in the set \mathcal{N} maintains its client-side model, denoted as $w_{c,n}$. These client-side models are trained in parallel using the clients' respective local datasets, through interactions with the server-side model w_s hosted on the main server. To synchronize the client-side models, clients participate in federated learning, coordinated by the fed server, to construct a global client-side model w_c in a collaborative manner [16].

Finally, the entire SFL process is carried out over T rounds. At the beginning of each round t , clients are provided with the latest global client-side model w_c from the fed server. Following this, both the clients and the main server engage in training over E epochs, updating their respective client-side models $w_{c,n}$ for each client $n \in \mathcal{N}$, and the server-side model w_s . Then, each client n randomly samples a mini-batch instance ζ_n from its dataset \mathcal{D}_n . Note that during each epoch, clients randomly partition their datasets into M mini-batches. Stochastic gradient descent (SGD) is applied to each mini-batch, allowing clients to update their client-side models $w_{c,n}$ and the main server to update the server-side model w_s in a coordinated fashion. Once the E epochs are concluded, the fed server collects the updated client-side models $w_{c,n}$ from all clients and combines them to form an updated global client-side model w_c^1 . A detailed timeline of overall SFL process is summarized in Fig. 2.

¹At mini-batch instance ζ_n , $l_n(w; \zeta_n)$ denotes the loss of the model w over client n 's mini-batch instance ζ_n , which can be expressed as follows:

$$l_n(w; \zeta_n) = h(w_s; u(w_{c,n}; \zeta_n)). \quad (1)$$

Here, u is a function on the client side that transforms the input data from the sampled mini-batch instance ζ_n into the activation space, producing the output of the client-side model $w_{c,n}$ (i.e., smashed data). Meanwhile, h is a function on the server side that takes the activation space as input and produces a single scalar value representing the loss.

A. Utility Function of SFL Model Owner

In our scenario, the SFL model owner determines the cut layer L_c and the incentives R provided to clients based on their data contributions, with the goal of maximizing the owner's utility function. In this context, we consider the following utility function:

$$U_{MO}(R, L_c, \mathbf{d}) = \tau_1 \ln \left(1 + \frac{\sum_{n=1}^N d_n}{d_{req}} \right) + \tau_2 \frac{f_{FLOPs}(L_c)}{w_{FLOPs}} - R, \quad (2)$$

where the vector $\mathbf{d} = (d_1, d_2, \dots, d_N)$ contains the data contribution of each client from its local dataset \mathcal{D}_n , while d_{req} denotes the required amount of aggregated data contribution necessary to achieve an acceptable accuracy, which is a service-dependent requirement. $\tau_1, \tau_2 \geq 0$ are weights for trading of the first and second terms. Moreover, w_{FLOPs} is the computation workload to proceed with the full model w during its forward and backward propagation for a single data sample, measured in Floating Point Operations Per Second (FLOPS). Here, $f_{FLOPs}(L_c)$ as a function of the computation workload, measured in FLOPS, of the client-side model w_c with respect to L_c . In this context, $f_{FLOPs}(L_c)$ is an increasing function of L_c since the computation workload increases with the number of layers. Nevertheless, due to the difficulty of analytically characterizing this model-dependency, a data-driven approach can be applied to model its relationship through offline training using empirical measurements. Hence, we adopt regression-based modeling, which is one of the most widely used approaches for modeling mobile CPU properties, such as CPU power and temperature variation modeling [17], [18]. Consequently, as shown in Fig. 3, we conclude that $f_{FLOPs}(L_c)$ is an affine function of L_c , modeled as $f_{FLOPs}(L_c) = aL_c + b$, where a and b are coefficient values². Finally, this utility function quantifies the balance between the satisfaction derived from aggregated data contribution from clients, and the gain from distributing training workload to clients, against the expenditure R allocated to clients during the SFL process. The range of R is set by the SFL model owner within $(0, R_{max}]$, where R_{max} represents the upper limit of incentives regulated by the SFL model owner's policy. Note that in the right-hand side of (2), the first term $\ln(1 + \frac{\sum_{n=1}^N d_n}{d_{req}})$ suggests that the satisfaction gained from aggregated data contribution may follow the law of diminishing returns. From [19], the amount of raw data plays an important role in the quality of data analytics (e.g., accuracy). Moreover, numerous studies demonstrate that model accuracy increases concavely with the overall dataset size [20]–[22]. Accordingly, a concave, strictly increasing, and continuously differentiable function can represent this term. In this paper, we adopt a logarithmic utility function for this purpose, as it is widely used in the literature to quantify user satisfaction with diminishing returns.

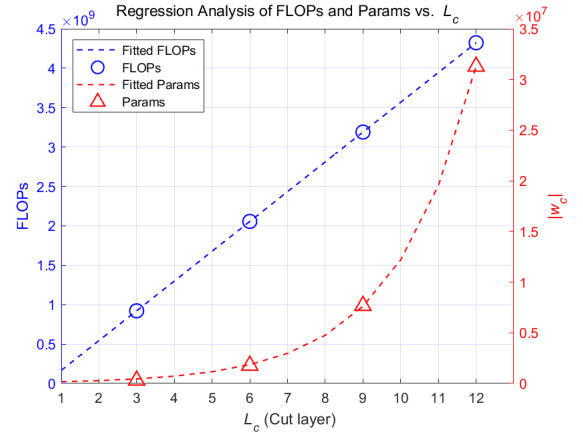


Fig. 3: Regression analysis of computation load and the number of model parameters with varying L_c .

B. Utility Function of Clients

Our design of the utility function for the clients comprises two terms. The first term denotes the incentive allocated by the SFL model owner, while the second term represents the energy expenditure incurred from participating in the SFL process.

1) *Overall computation energy of the client:* Using $f_{FLOPs}(L_c)$ to model the computation time for each client n , we obtain computation latency for the client-side model to process the mini-batch instance ζ_k can be obtained by

$$t_n = \frac{d_n f_{FLOPs}(L_c)}{M f_n \kappa}, \quad \forall n \in \mathcal{N}, \quad (3)$$

where the size of the mini-batch instance ζ_k is denoted by $|\zeta_k| = d_n/M$. Furthermore, f_n denotes the central processing unit (CPU) capability of client n , and κ represents the computing intensity. Consequently, the energy consumption for computing the client-side model for client n is given by $E_{cmp,n} = p_n^c t_n$, where p_n^c is the computation power of client n .

2) *Overall communication energy of the client:* To streamline our analysis and focus on the core intuition, we adopt a simplified approach similar to [23]. This involves assuming fixed uplink and downlink channels, maintaining a quasi-static channel mode throughout the SFL process facilitating efficient analysis. Then, transmission latencies for transmitting the smashed data from client n to the main server and for receiving the gradient data from the main server to the client n , are given by:

$$t_{s:n} = \frac{s_n}{r_{s:n}}, \quad t_{g:n} = \frac{g_n}{r_{g:n}}, \quad \forall n \in \mathcal{N}. \quad (4)$$

Here, s_n and g_n denote the size of the smashed data and the gradient data of client n , respectively³. Additionally, $r_{s:n}$ and $r_{g:n}$ represent the uplink transmission rate from client n to the main server and the downlink transmission rate from the main server to client n , respectively. Similarly, transmission latencies for transmitting the client-side model from client n

²We used the thop package to measure the forward FLOPs and the model Params: <https://pypi.org/project/thop/>. Backward FLOPs are assumed to be twice the forward FLOPs.

³Here, we assume that the size of the smashed data is constant, although it could be model-dependent. For the evaluation, we set the size of the smashed data by averaging the size across layers to simplify the analysis.

to the fed server and for receiving the global client-side model from the fed server to the client n , are given by:

$$t_{cm:n} = \frac{m|w_c|}{r_{cm:n}}, \quad t_{gcm:n} = \frac{m|w_c|}{r_{gcm:n}}, \quad \forall n \in \mathcal{N}. \quad (5)$$

Here, $r_{cm:n}$ and $r_{gcm:n}$ represent the uplink transmission rate from client n to the fed server and the downlink transmission rate from the fed server to client n , respectively. m represents the number of bits for a single model parameter, where $|w_c|$ is the total number of model parameters in the client-side model. Note that the size of the global client-side model is the same as that of the individual client-side model. In this context, $|w_c|$ is the function of L_c since the number of model parameters increases with the number of layers. Similar to f_{FLOPs} , due to the difficulty of analytical modeling, we also adopted regression-based modeling. Consequently, as shown in Fig. 3, we conclude that $|w_c|$ is a convex function of L_c , modeled as $|w_c| = c \exp(dL_c)$, where c and d are coefficient values. Then, with given p_n^t and p_n^r of transmission and receiving power consumption of client n , the overall communication energy for interacting with main server $E_{com-m:n}$ and fed server $E_{com-f:n}$ can be calculated by

$$E_{com-m:n} = p_n^t t_{s:n} + p_n^r t_{g:n}, \quad \forall n \in \mathcal{N}. \quad (6)$$

$$E_{com-f:n} = p_n^t t_{cm:n} + p_n^r t_{gcm:n}, \quad \forall n \in \mathcal{N}. \quad (7)$$

3) *Overall energy consumption*: The energy consumption for E epochs of client n with M mini-batches is given by $E_n^{epoch} = EM(E_{cmp,n} + E_{com-m,n})$, $n \in \mathcal{N}$. Consequently, the overall energy consumption for T rounds, covering the entire duration until the SFL system completes its operations, is given by

$$E_{tot,n} = T(E_n^{epoch} + E_{com-f:n}), n \in \mathcal{N}. \quad (8)$$

Then, in order to demonstrate the influence of L_c and d_n on $E_{tot,n}$, (8) can be simplified as

$$E_{tot,n} = T((d_n f_{FLOPs}(L_c) A_n + B_n) + c \exp(dL_c) C_n), n \in \mathcal{N}, \quad (9)$$

where $A_n = E \frac{p_n^c}{f_n \kappa}$, $B_n = EM E_{com-m,n}$, and $C_n = \frac{m p_n^t}{r_{cm:n}} + \frac{m p_n^r}{r_{gcm:n}}$. Similarly, (9) can be further simplified to highlight only the impact of d_n on $E_{tot,n}$, which is given by

$$E_{tot,n} = d_n H_n + I_n, n \in \mathcal{N}, \quad (10)$$

where $H_n = T f_{FLOPs}(L_c) A_n$ and $I_n = T(B_n + C_n c \exp(dL_c))$.

4) *Shared incentives and utility function design*: Adhering to the principle of proportional sharing, the SFL model owner allocates an amount of incentives R to each client $n \in \mathcal{N}$ in proportion to their data contributions. Accordingly, the specific amount of incentives R_n allocated to client n by the SFL model owner is determined as

$$R_n = R \frac{d_n}{\sum_{l=1}^N d_l}. \quad (11)$$

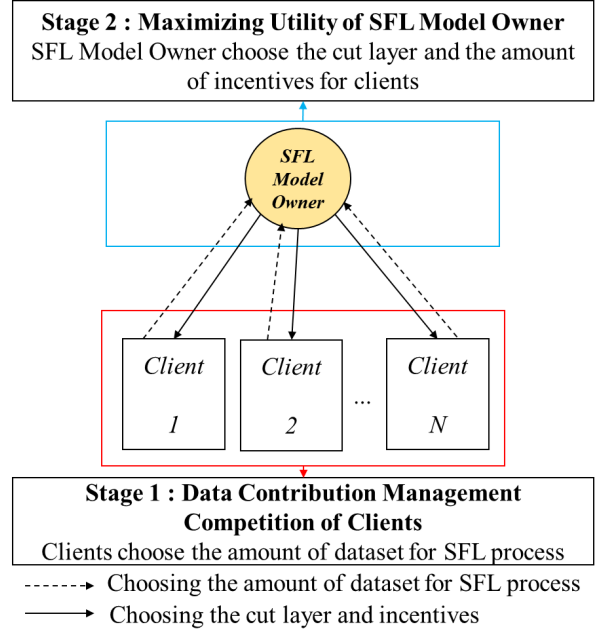


Fig. 4: A diagram of a two-stage Stackelberg game in SFL where the SFL model owner is a leader and clients are followers.

Thus, the utility function of client n is given by

$$U_n(\mathbf{d}, R, L_c) = \psi_n R_n - E_{tot,n} + S, \\ = \psi_n R \frac{d_n}{\sum_{l=1}^N d_l} - d_n H_n - I_n + S, \quad (12)$$

where $\psi_n (> 0)$ is a weighting factor for the incentives of client n . And S is an offset to U_n as a baseline constant term, representing the satisfaction of clients using the SFL model.

IV. GAME-THEORETIC ANALYSIS

In this section, we examine the competitive dynamics between the SFL model owner and the clients, while also considering the competition among clients to gain more incentives. These competitive behaviors can be considered as a hierarchical noncooperative decision problem, analyzable as a Stackelberg game. Stackelberg games are a type of noncooperative game characterized by a hierarchy among players, in which they are classified as leaders and followers [24]–[26]. In this study, we consider a scenario where the clients follow the behavior of the SFL model owner. Treating the SFL model owner as the leader and the clients as the followers, the competition among players to maximize their utilities is modeled as a two-level Stackelberg game. If the SFL model owner decides on the cut layer and the total amount of incentives, the clients will respond by selecting their optimal strategies regarding data contribution for the SFL process. The SFL model owner is aware that the clients will choose their best response strategies based on the owner's decisions. Therefore, the SFL model owner optimizes its strategy to maximize utility, taking into account the clients' best responses. To find the Stackelberg Equilibrium (SE), which is the solution to this game, we employ a backward induction technique

introduced in [24], [25]. As illustrated in Fig. 4, this technique can be summarized as follows. First, in the lower-level game for the clients, referred to as Stage 1: Data Contribution Management Competition, the clients determine the amount of data to contribute to maximize their utility function (12), given the incentives and cut layer configuration. Then, in the upper-level game for the SFL model owner, referred to as Stage 2: Maximizing Utility of SFL Model Owner, the SFL model owner combines the clients' strategies with its utility function (2) and selects the cut layer and incentive amounts that maximize its own utility function (2).

A. Stage 1: Noncooperative Game Among Clients

Each client aims to maximize its utility function (12) within the dataset constraints $[0, D_n]$. Given the vector $\mathbf{d} = (d_1, d_2, \dots, d_N)$, let \mathbf{d}_{-n} denote the profile of strategies for the clients except n , i.e., $\mathbf{d}_{-n} = (d_l)_{l \in \mathcal{N} \setminus \{n\}}$. Then, by definition, we have $\mathbf{d} = (d_n, \mathbf{d}_{-n})$.

Note that, to simplify the problem, we relax the integer variable d_n into a continuous variable. Thus, the optimization problem to find the optimal amount of data contribution for the SFL process is given by

$$\underset{d_n}{\text{maximize}} \quad U_n(\mathbf{d}, R, L_c) \quad (13)$$

$$\begin{aligned} & \text{subject to} \\ & 0 \leq d_n \leq D_n, \text{ for } n \in \mathcal{N}. \end{aligned}$$

Definition 1. The best response (BR) function $B_n(\mathbf{d}_{-n}, R, L_c)$ of client n as a follower is the best strategy for client n given the other clients' strategies \mathbf{d}_{-n} and SFL model owner strategies R and L_c . The BR function is denoted as follows:

$$B_n(\mathbf{d}_{-n}, R, L_c) = \arg \max_{d_n} U_n(d_n, \mathbf{d}_{-n}, R, L_c) \text{ for } n \in \mathcal{N}. \quad (14)$$

Definition 2. A Nash equilibrium of the noncooperative game among the clients is a profile of strategies $\mathbf{d}^* = (d_1^*, d_2^*, \dots, d_N^*)$ with the property that, given the SFL model owner strategies R , and L_c , we obtain

$$d_n^* = B_n(\mathbf{d}_{-n}, R, L_c), \text{ for } n \in \mathcal{N}. \quad (15)$$

Theorem 1. The utility function $U_n(d_n, \mathbf{d}_{-n}, R, L_c)$ of client n is strictly concave in d_n . Thus, a Nash equilibrium exists in the noncooperative game among the clients.

Proof. Taking the first and second derivatives of $U_n(d_n, \mathbf{d}_{-n}, R, L_c)$ with respect to d_n , we obtain

$$\frac{\partial U_n(d_n, \mathbf{d}_{-n}, R, L_c)}{\partial d_n} = \psi_n R \frac{\sum_{l \in \mathcal{N} \setminus \{n\}} d_l}{(\sum_{l=1}^N d_l)^2} - H_n, \quad (16)$$

$$\frac{\partial^2 U_n(d_n, \mathbf{d}_{-n}, R, L_c)}{\partial d_n^2} = -2\psi_n R \frac{\sum_{l \in \mathcal{N} \setminus \{n\}} d_l}{(\sum_{l=1}^N d_l)^3} < 0, \quad (17)$$

It follows from (17) that the second derivatives of the utility function U_n is negative. This implies that the utility function $U_n(d_n, \mathbf{d}_{-n}, R, L_c)$ is strictly concave in d_n where

the dataset constraints $[0, D_n]$ is a compact and convex set. Thus, the proposed noncooperative client-level game has a Nash equilibrium [27]. ■

Definition 3. A function $f(p) = (f_1(p), \dots, f_N(p))$, where $p = (p_1, \dots, p_N)$, is said to be standard if the following properties are satisfied for all $p \geq 0^4$.

- Positivity : $f(p) > 0$.
- Monotonicity : For all p and p' , if $p \geq p'$, then $f(p) \geq f(p')$.
- Scalability : For all $\mu > 1$, $\mu f(p) > f(\mu p)$.

To prove the uniqueness of the Nash equilibrium in the proposed client-level game, it is sufficient to demonstrate that the BR function of each client, as defined in (15), is a standard function [27].

Theorem 2. The BR function $B_n(\mathbf{d}_{-n}, R, L_c)$ of client n is a standard function of \mathbf{d}_{-n} for sufficiently large R .

Proof. By equating the first derivative of $U_n(d_n, \mathbf{d}_{-n}, R, L_c)$ in (16) to zero, we obtain

$$\psi_n R \frac{\sum_{l \in \mathcal{N} \setminus \{n\}} d_l}{(\sum_{l=1}^N d_l)^2} = H_n.$$

Then, solving the above equation, we have

$$\begin{aligned} d_n &= \sqrt{\frac{\psi_n R \sum_{l \in \mathcal{N} \setminus \{n\}} d_l}{H_n}} - \sum_{l \in \mathcal{N} \setminus \{n\}} d_l \\ &= \sqrt{\sum_{l \in \mathcal{N} \setminus \{n\}} d_l} \left(\sqrt{\frac{\psi_n R}{H_n}} - \sqrt{\sum_{l \in \mathcal{N} \setminus \{n\}} d_l} \right). \end{aligned} \quad (18)$$

Additionally, if the expression on the right-hand side of (18) exceeds D_n , the client n will participate by setting $d_n = D_n$.

Consequently, the BR function $B_n(\mathbf{d}_{-n}, R, L_c)$ (also denoted as d_n^*) is given as follows:

$$d_n^* = \begin{cases} 0 & , \text{ if } \frac{\psi_n R}{H_n} \leq \sum_{l \in \mathcal{N} \setminus \{n\}} d_l, \\ (18) & , \text{ if } 0 < d_n < D_n, \\ D_n & , \text{ otherwise} \end{cases} \quad (19)$$

- Positivity: Under the condition $\frac{\psi_n R}{H_n} > \sum_{l \in \mathcal{N} \setminus \{n\}} d_l$, we obtain

$$B_n(\mathbf{d}_{-n}, R, L_c) > 0.$$

- Monotonicity : Under the same condition, by taking the first derivatives of $B_n(\mathbf{d}_{-n}, R, L_c)$ with respect to d_l for $l \in \mathcal{N} \setminus \{n\}$, we obtain

$$\frac{\partial B_n(\mathbf{d}_{-n}, R, L_c)}{\partial d_l} = \frac{1}{2} \sqrt{\frac{\psi_n R}{H_n}} \frac{1}{\sqrt{\sum_{l \in \mathcal{N} \setminus \{n\}} d_l}} - 1.$$

If we extend the positivity condition to $\frac{\psi_n R}{H_n} > 4 \sum_{l \in \mathcal{N} \setminus \{n\}} d_l$, this still implies the necessity of providing sufficient R for clients. The aforementioned first derivatives of $B_n(\mathbf{d}_{-n}, R, L_c)$ satisfy the positivity, indicating that it is an increasing function.

⁴Here, $p \geq 0$ indicates that p is elementwise non-negative, i.e., $p_i \geq 0$ for all $i = 1, \dots, N$.

- Scalability : From (18), we have

$$\begin{aligned} & \mu B_n(\mathbf{d}_{-n}, R, L_c) \\ &= \mu \left(\sqrt{\frac{\psi_n R \sum_{l \in \mathcal{N} \setminus \{n\}} d_l}{H_n}} - \sum_{l \in \mathcal{N} \setminus \{n\}} d_l \right) \end{aligned}$$

and

$$\begin{aligned} & B_n(\mu \mathbf{d}_{-n}, R, L_c) \\ &= \sqrt{\frac{\psi_n R \mu \sum_{l \in \mathcal{N} \setminus \{n\}} d_l}{H_n}} - \mu \sum_{l \in \mathcal{N} \setminus \{n\}} d_l. \end{aligned}$$

Because $\mu > 1$, we obtain

$$\begin{aligned} & \mu B_n(\mathbf{d}_{-n}, R, L_c) - B_n(\mu \mathbf{d}_{-n}, R, L_c) \\ &= \sqrt{\mu}(\sqrt{\mu} - 1) \sqrt{\frac{\psi_n R}{H_n} \sum_{l \in \mathcal{N} \setminus \{n\}} d_l} > 0. \end{aligned}$$

Under the condition $\frac{\psi_n R}{H_n} > 4 \sum_{l \in \mathcal{N} \setminus \{n\}} d_l$ implying that the sufficient R is provided for clients, we can conclude that the BR function $B_n(\mathbf{d}_{-n}, R, L_c)$ is a *standard function* of \mathbf{d}_{-n} . ■

Theorem 3. *The non-cooperative game among the clients has a unique Nash equilibrium.*

Proof. Referring to Theorem 2, we can verify whether the BR function $B_n(\mathbf{d}_{-n}, R, L_c)$ conforms to the definition of a *standard function*. This in turn ensures the uniqueness of the fixed point $\mathbf{d}^* = (d_1^*, d_2^*, \dots, d_N^*)$. ■

Theorem 4. *For the noncooperative game among clients, the unique Nash equilibrium has a closed-form expression given by the following:*

$$d_n^* = \frac{(N-1)R}{\sum_{l \in \mathcal{N}} \frac{H_l}{\psi_l}} \left(1 - \frac{H_n(N-1)}{\psi_n \sum_{l \in \mathcal{N}} \frac{H_l}{\psi_l}} \right) \quad \forall n \in \mathcal{N}, \quad (20)$$

where d_n^* should satisfy the constraint of $[0, D_n]$ as specified in (19).

Proof. From (19), for any client $n \in \mathcal{N}$, we obtain

$$\sum_{l \in \mathcal{N}} d_l^* = \sqrt{\frac{\psi_n R \sum_{l \in \mathcal{N} \setminus \{n\}} d_l^*}{H_n}}. \quad (21)$$

By setting $\eta = \sum_{l \in \mathcal{N}} d_l^*$, we can derive that

$$d_n^* = \eta - \frac{\eta^2 H_n}{\psi_n R}. \quad (22)$$

By summing (22) over N clients, we have

$$\eta = N\eta - \frac{\eta^2}{R} \sum_{l \in \mathcal{N}} \frac{H_l}{\psi_l}. \quad (23)$$

By solving the problem of (23), we obtain

$$\eta = \frac{(N-1)R}{\sum_{l \in \mathcal{N}} \frac{H_l}{\psi_l}}. \quad (24)$$

By substituting (24) into (22), we derive the closed-form expression in (20). ■

B. Stage 2: Utility Maximization for SFL Model Owner

The optimization problem for the SFL model owner is formulated as

$$\begin{aligned} & \underset{R, L_c}{\text{maximize}} \quad U_{MO}(R, L_c, \mathbf{d}^*) \\ & \text{subject to} \\ & R_{\min} \leq R \leq R_{\max} \ \& \ L_{\min} \leq L_c \leq L_{\max}, \end{aligned} \quad (25)$$

where \mathbf{d}^* is given by (20). Note that, to simplify the problem, we relax the integer variables R and L_c into continuous variables. In this context, R_{\min} and R_{\max} in the constraints can be set by the SFL model owner as the minimum requirement to motivate the SFL participants and as the maximum reward for attempting to achieve a positive utility value, respectively, by balancing the three terms in U_{MO} , taking their weighting factors into account. Moreover, L_{\min} and L_{\max} can be set by the SFL model owner to ensure that privacy concerns from clients (e.g., reconstruction attacks) are not violated and to avoid imposing excessive burdens on clients during the SFL process, respectively.

Theorem 5. *An optimal solution for R and L_c exists for maximizing the utility function $U_{MO}(R, L_c, \mathbf{d}^*)$.*

Proof. Since d_n^* in (20) is a linear function of R , we can redefine it as

$$d_n^* = X_n(L_c)R, \quad (26)$$

where X_n is a function of L_c that acts as the coefficient in the linear function specifying d_n^* . Then, by substituting (26) into U_{MO} , then U_{MO} is given by

$$\begin{aligned} & U_{MO}(R, L_c, \mathbf{d}^*) \\ &= \tau_1 \ln\left(1 + R \frac{\sum_{n=1}^N X_n(L_c)}{d_{req}}\right) + \tau_2 \frac{f_{FLOPs}(L_c)}{w_{FLOPs}} - R. \end{aligned}$$

Finally, for any feasible R and L_c , taking the second derivatives of U_{MO} with respect to R and L_c , we have

$$\frac{\partial^2 U_{MO}}{\partial R^2} = -\frac{\tau_1 (\sum_{n=1}^N X_n(L_c))^2}{d_{req}^2 (1 + R \frac{\sum_{n=1}^N X_n(L_c)}{d_{req}})^2} < 0. \quad (27)$$

Accordingly, U_{MO} is strictly concave with respect to R with given $X_n(L_c)$. Then, the optimal R^* can be determined using a CVX solver. On the other hand, demonstrating the concavity of the function $X_n(L_c)$ with respect to L_c analytically is challenging. Therefore, within the constraints from L_{\min} to L_{\max} , we can find the optimal solution of R^* and L_c^* using the exhaustive search-based heuristic algorithm with the CVX solver described in Algorithm 1. This approach is reasonable because the search space of L_c is relatively small, making it practically deployable. ■

Theorem 6. *A Stackelberg equilibrium exists in the proposed two-stage Stackelberg game in SFL.*

Algorithm 1 Find optimal L_c and R
Input : \mathbf{d}^*
Output : Optimal L_c, R

- 1: **Initialize** $\mathbf{M}[1, \dots, L_{\max}]$ with $-Inf$
- 2: **for** L_c from L_{\min} to L_{\max} **do**
- 3: $R \leftarrow$ solve (25) by using a CVX solver
- 4: $\mathbf{M}[L_c] \leftarrow U_{MO}(R, L_c, \mathbf{d}^*)$
- 5: **end for**
- 6: $(R^*, L_c^*) \leftarrow \text{argmax}(\mathbf{M})$
- 7: **Return** (R^*, L_c^*)

TABLE I: Parameter Settings

Parameters	Values
N	5
M	100
d_{req}	2,000
m	32
s_n, g_n	24.5 Mbits
$r_{s:n}, r_{cm:n}$	100 Mbit/s
$r_{g:n}, r_{gcm:n}$	200 Mbit/s
w_{FLOPs}	4.3 GFLOPs
κ	16 FLOPs/cycle
p_n^c	4 W
p_n^t, p_n^r	0.2 W

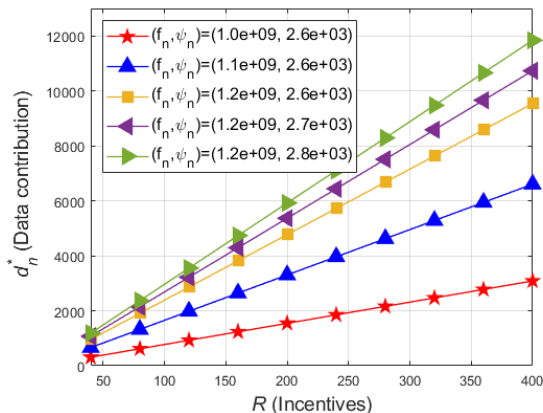
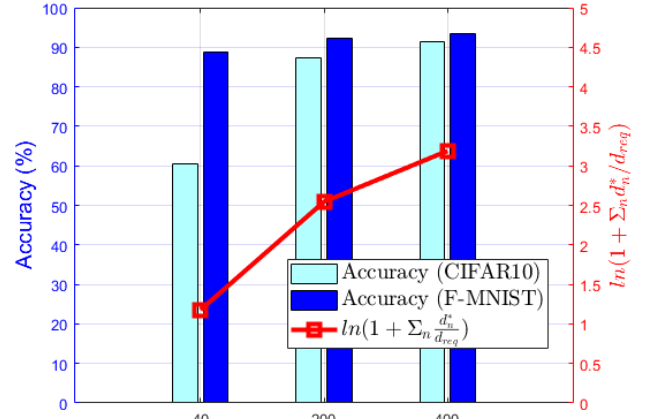
Proof. Because the noncooperative game among the clients has a unique Nash equilibrium $\mathbf{d}^* = (d_1^*, d_2^*, \dots, d_N^*)$, as shown in Theorem 4, and the SFL model owner can always find its optimal strategy R^* and L_c^* , as shown in Theorem 5, we conclude that a Stackelberg equilibrium exists in the proposed two-stage Stackelberg game in SFL. ■

V. PERFORMANCE EVALUATION

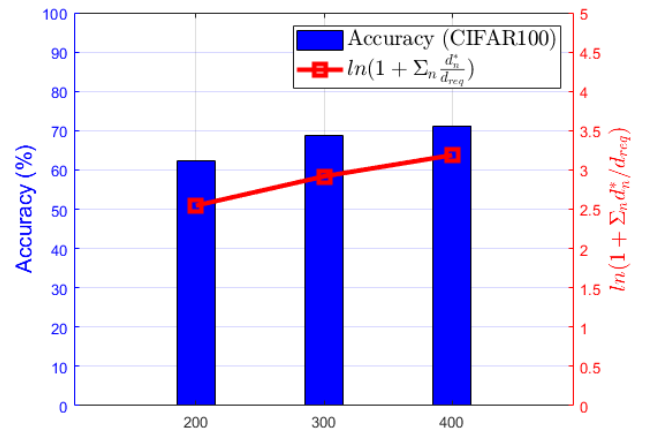
This section presents experimental results from our game-theoretic analysis of SFL, involving the SFL model owner and

TABLE II: Regression-Based Models

	Proposed Models	RMSE
$GFLOPs$	$f_{FLOPs}(L_c) = 0.3779 \cdot L_c - 0.212$	0.0004
$MParams$	$ w_c = 0.1098 \cdot \exp(0.4711 \cdot L_c)$	0.0909


 Fig. 5: Data contribution at NE for various (f_n, ψ_n) pairs.


(a) F-MNIST/CIFAR10



(b) CIFAR100

Fig. 6: Model accuracy and satisfaction at SE.

the clients. The detailed simulation parameters and regression-based models are specified in Tabs. I and II.

We begin by examining the optimal data contribution d_n^* from the n -th client at the Nash Equilibrium (NE). For given incentive values R , the client data contributions are derived from (19) and (20), as stated in **Theorem 4**. For this numerical analysis, we assume that the cut layer is set at $L_c = 3$, and five heterogeneous clients have CPU capabilities $f_n = [1.0, 1.1, 1.2, 1.2, 1.2]$ GHz, with corresponding incentive weighting factors $\psi_n = [2.6, 2.6, 2.6, 2.7, 2.8] \times 10^3$, respectively. Fig. 5 shows the results for R in the range $[40, 400]$. As expected, incentive R increases the data contribution d_n^* by encouraging clients to participate more actively in SFL process. Interestingly, d_n^* diminishes as the CPU capability f_n of participating clients increases, suggesting a strategic balance between data contribution and energy consumption, as modeled in (12). This is because clients with higher CPU capabilities tend to reduce execution times more, balancing the trade-off between earning incentives and minimizing energy consumption. Notably, among clients with identical CPU capabilities, those with higher incentive weighting factors ψ_n

tend to contribute more data.

To keep the experiment manageable with classification accuracy based on data contributions, we further assume homogeneity among the five clients, with each having $f_n = 1.2$ GHz and $\psi_n = 2.8 \times 10^3$. For this analysis, we conducted classification experiments under Independent and Identically Distributed (IID) data settings using two datasets, the CIFAR-10 dataset [28] and Fashion-MNIST [29] to evaluate SFL accuracy according to the data contribution. The CIFAR-10 dataset comprises color images with 10 object categories, with 50,000 and 10,000 samples in training and test splits. The Fashion-MNIST dataset comprises grayscale images categorized into 10 distinct fashion classes, with 60,000 samples for the training split and 10,000 samples for the test set. To ensure consistency in the number of training samples between Fashion-MNIST and CIFAR-10 datasets, we utilized 50,000 samples for the training set from the Fashion-MNIST training split. This adjustment facilitates a direct comparison of accuracy trends between the two datasets, enabling a consistent evaluation of classification accuracy in relation to data contributions. Data from the training split were allocated among five clients proportionate to their data contributions d_n^* , which were determined by incentive values R . Specifically, in scenarios with incentives of 40, 200, and 400, each client contributes 900, 4700, and 9300 samples, respectively, totaling 4,500, 23500, and 46,500 samples were used for SFL training in each scenario. The model evaluation employed all 10,000 samples from the test split. The SFL model w is structured with 12 convolutional blocks (Conv-BN-ReLU), incorporating Max Pooling every third block, followed by two fully connected layers, a dropout layer, and a Softmax output layer. The model split between client and server was determined at cut layers after the convolution blocks, offering 12 viable points for split. Input images were normalized using predefined means and standard deviations (mean=[0.4914, 0.4822, 0.4465], std=[0.2023, 0.1994, 0.2010]), and data augmentation techniques such as random cropping and horizontal flipping were applied. An Adam optimizer facilitated the training, set to a learning rate of 0.0001 and beta values of (0.5, 0.999). Model training hyper-parameters are detailed in Tab I. The SFL outcomes, displayed in Fig. 6a, align with those observed in Fig. 5, affirming the critical role of raw data volume in model quality and accuracy, as discussed in [19]. To enhance the generalizability of these findings, we extended our experiments to the CIFAR-100 dataset [28], which is similar to CIFAR-10 but consists of 100 object categories. The dataset is divided into 50,000 training samples and 10,000 test samples. Since datasets with larger numbers of categories generally require more training data to achieve stable model training, we set the incentives R to 200, 300, and 400. This resulted in each client contributing 4,700, 7,000, and 9,300 samples, respectively. Consequently, the SFL model in the CIFAR-100 scenario was trained using a total of 23,500, 35,000, and 45,000 samples. Figure 6b illustrates that the conclusions drawn for CIFAR-10 remain consistent in the CIFAR-100 setting. The results obtained from the CIFAR-100 dataset also confirm that the observed consistency in classification accuracy is independent of the dataset type. It is recommended for the SFL model

owner to employ a Stackelberg strategy, where incentives are distributed proportionately to the clients' CPU capabilities, thus accelerating SFL and enhancing model accuracy.

Continuing, we examine scenarios involving an increased number of homogeneous clients, each characterized by CPU capabilities of $f_n = 1.2$ GHz and incentive weighting factors $\psi_n = 2.8 \times 10^3$. The optimization constraints in (25) L_{\min} , L_{\max} , R_{\min} , and R_{\max} are set to 3, 12, 60, and 1,000, respectively. Fig. 7 shows the numerical outcomes for various settings of $\frac{\tau_1}{\tau_2}$ ratio. Fig. 7a indicates that increasing the number of clients necessitates higher incentives, as the incentive R is proportionally distributed among the clients according to their data contributions, as described in (12). Additionally, an elevated τ_2 compared to τ_1 (i.e., lower ratio τ_1 to τ_2) reflects the SFL model owner's strategy to minimize the server's computational burden, resulting in the maximal cut layer value $L_c = 12$ and a correspondingly lower R^* . In contrast, an increased τ_1 , enhancing data contribution, leads to an increase in the optimal R^* and maintaining the minimal cut layer $L_c = 3$ to encourage active client participation. These observations are further corroborated by additional analysis of the utility functions of the SFL model owner U_{MO} and clients U_n . As shown in Fig. 7b, the utility trends of U_{MO} for the SFL model owner are consistent with Fig. 7a, whereas the pattern in Fig. 7c contrasts with these⁵. It becomes evident that as more clients engage in SFL, their utility U_n diminishes. Specifically, a higher ratio of τ_1 to τ_2 distinctly leads to reduced utility for the number of clients, confirming the inverse relationship highlighted in Fig. 7c.

Finally, we evaluated the efficiency of a noncooperative game among clients, which is degraded due to their selfish behavior in the absence of central coordination. This efficiency is measured by the price of anarchy (PoA) $[1, \infty)$, defined as the ratio between the optimal centralized solution and the worst equilibrium in games with multiple equilibria. In our case, since our problem has a unique NE, the PoA is given by

$$PoA = \frac{\underset{d_n}{\text{maximize}} \sum_{n=1}^N U_n(\mathbf{d}, R, L_c)}{\sum_{n=1}^N U_n(\mathbf{d}^*, R, L_c)}. \quad (28)$$

As illustrated in Fig. 8, the PoA decreases as the number of clients increases⁶. This trend confirms that the NE of the noncooperative game becomes more effective with a larger number of clients. This occurs because, as the number of clients increases, the optimal data contribution \mathbf{d}^* at NE decreases. The elevated competition among a larger number of clients reduces expected individual incentives, thereby narrowing the gap between the optimal centralized solution and the NE. Additionally, as shown in Fig. 9, the PoA also decreases with an increase in L_c . This occurs because a higher L_c places a greater burden on clients, leading to a reduction of \mathbf{d}^* at NE. Consequently, L_c can be an effective regulator for controlling the effectiveness of the NE by adjusting the level of competition.

⁵When plotting this graph, we set the baseline constant term S to 10^6 to ensure U_n is greater than zero.

⁶We set the minimum required d_n as d_{req}/N to ensure that the aggregated data contribution meets the minimum necessary amount for acceptable accuracy in SFL.

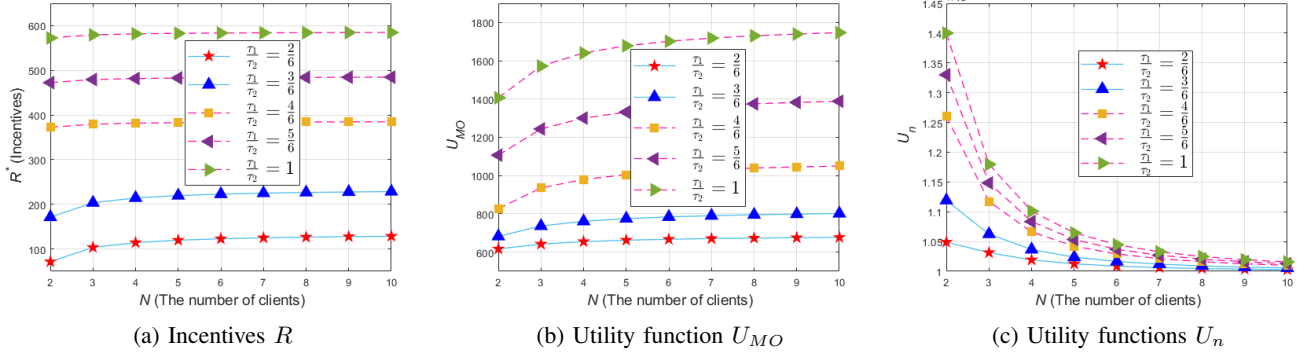


Fig. 7: (a) Incentives at NE and (b)-(c) Utility functions at SE for various $\frac{T_1}{T_2}$ ratios. (For the dotted line, the cut layer L_c^* was selected as L_{min} , whereas for the solid line, it was chosen as L_{max} .)

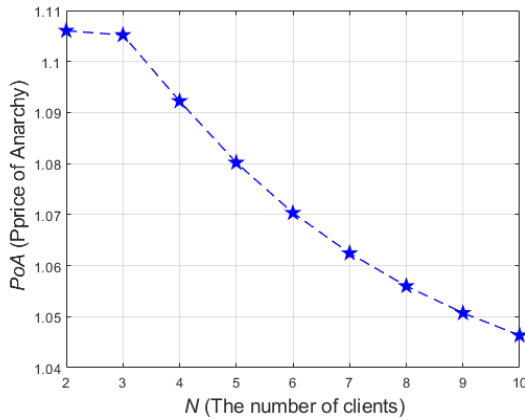


Fig. 8: PoA vs. the number of clients ($\psi_n=2800$)

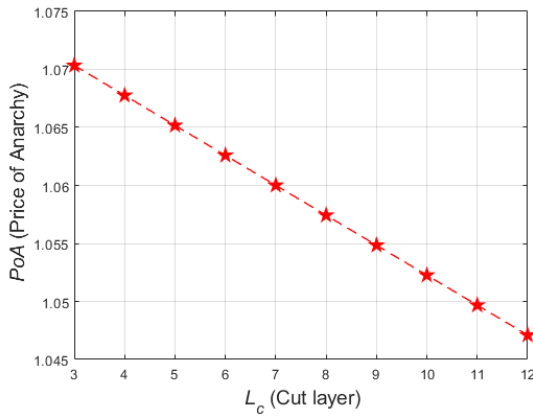


Fig. 9: PoA vs. varying L_c ($N = 6$)

We also validated a balance between utility and classification accuracy by comparing the proposed method with other approaches, as illustrated in Fig. 10. Under the conditions $N = 5$ and $\frac{T_1}{T_2} = \frac{4}{6}$, the proposed method determined the optimal incentive and cut layer to be $R^* = 382.85$ and $L_c^* = 3$, respectively. This configuration resulted in each client contributing 9,000 training samples, with a total of 45,000 samples across all five clients in the CIFAR-10

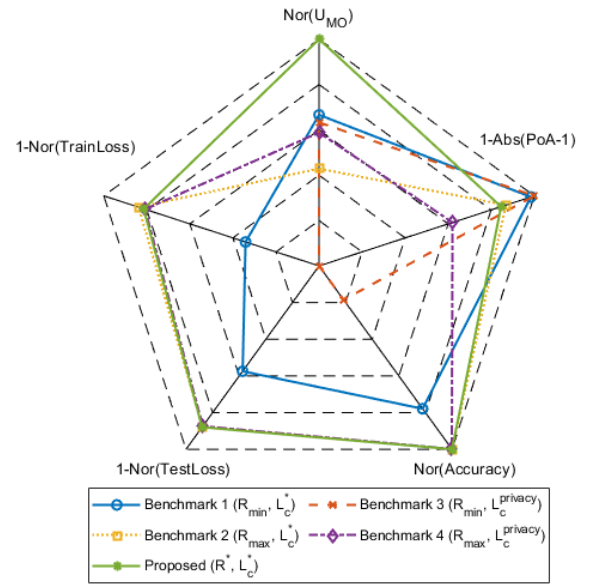


Fig. 10: Comparison of normalized utility, PoA, and performance metrics. Normalization is defined as $Nor(a) = a/\max(a)$ and $Abs(a) = |a|$ represents the absolute value. The larger the pentagon, the better.

dataset. The impact of the incentive R was analyzed through two benchmarks: Benchmark 1, defined as (R_{min}, L_c^*) , and Benchmark 2, defined as (R_{max}, L_c^*) , where L_c^* is the same cut layer obtained by the proposed method. With $R_{min} = 60$, each client contributed $d_n^* = 1,400$ data samples, while R_{max} yielded $d_n^* = 23,330$ samples per client. However, due to the CIFAR-10 dataset's constraints, the maximum number of samples per client was limited to 10,000. The effect of the cut layer was further evaluated using Benchmark 3 and Benchmark 4, defined as $(R_{min}, L_c^{privacy})$ and $(R_{max}, L_c^{privacy})$, respectively. In these cases, $L_c^{privacy} = 8$ was selected to mitigate privacy leakage, as choosing a higher cut layer helps reduce privacy leakage, a concept that will be discussed later.

The proposed method and all benchmarks 1 to 4 were compared across five measures: utility of the SFL model owner (U_{MO}), price of anarchy (PoA), Accuracy, TestLoss,

and TrainLoss. Each measure was normalized using $\text{Nor}(a) = \frac{a}{\max(a)}$, with $\text{Abs}(a) = |a|$ representing the absolute value. Fig. 10 presents the normalized comparison of utility, PoA, accuracy, and loss values, where a larger pentagon plot signifies better overall performance. As demonstrated by the previous experiments, larger training datasets lead to improve accuracy, indicating R_{\max} maximizes accuracy (Benchmarks 2 and 4). However, when R_{\max} is applied, this also results in a side effect of reduced U_{MO} . Furthermore, R_{\max} also significantly increases data requirements and training complexity. An increased L_c causes clients to contribute fewer data samples, which in turn degrades classification accuracy. (Benchmark 3) In contrast, the proposed method successfully balanced R^* and L_c^* , optimizing both utility and accuracy. The optimal $R^* = 382.85$ determined by the proposed method requires only $d_n^* = 9,000$ samples per client, achieving comparable performance to R_{\max} case while offering improved utility (U_{MO}) for the SFL model owner.

Finally, efficiency was assessed using the PoA, where values closer to 1 indicate greater efficiency. As shown in Fig. 10, Benchmarks 1 and 3 achieve the highest PoA, but this comes with the sacrifice of reduced classification accuracy due to R_{\min} . The proposed method achieved a PoA closer to 1 than Benchmark 2 and Benchmark 4 (R_{\max}). We can conclude that the proposed method effectively balances R and L_c , achieving both optimal utility and accuracy.

VI. DISCUSSION

A. Impact of Cut Layer Selection on Privacy

In SFL, the main server can still potentially reconstruct the original input data from the smashed data (specifically, the embedded features) received from clients, a vulnerability known as a reconstruction attack. This risk is particularly relevant if the main server is honest but curious (HBC). From the study [14], we found that the selection of the cut layer significantly impacts the privacy level. For example, as the cut layer L_c increases, indicating greater model complexity, the quality of the reconstructed image decreases. This degradation in image quality corresponds to enhanced privacy because the increased complexity of the client-side model introduces advanced nonlinearities into the output. Therefore, to address client concerns regarding privacy, the SFL model owner should carefully select L_{\min} to ensure an acceptable level of privacy.

B. Interplay between Cut Layer Selection and Differential Privacy

Clients can enhance their privacy by proactively adding noise to the smashed data, a technique known as differential privacy (DP). Here, the amount of noise added is inversely proportional to the privacy leakage parameter ϵ . Formally, let D represent a set of data points, and \mathcal{M} be a probabilistic function or mechanism acting on databases. The mechanism \mathcal{M} is considered (ϵ, δ) -DP if, for all subsets of possible outputs $S \subseteq \text{Range}(\mathcal{M})$, and for all pairs of databases D and D' that differ by a single element, the following condition holds:

$$\Pr(\mathcal{M}(D) \in S) \leq e^\epsilon \Pr(\mathcal{M}(D') \in S) + \delta, \quad (29)$$

TABLE III: Accuracy and SSIM with varying noise level (σ)

	Cut layer	$\sigma = 0$	$\sigma = 1$	$\sigma = 2$
Accuracy	$L_c = 3$	90.8	90.1	88.0
	$L_c = 12$	92.1	91.8	92.0
Privacy Leakage (SSIM)	$L_c = 3$	0.9563	0.7692	0.5194
	$L_c = 12$	0.2721	0.1606	0.0921

where the smaller values of ϵ and δ indicate higher levels of privacy and vice versa. The essence of this definition is that when a client's data is added to or removed from the database, the distribution of outcomes from a private mechanism should remain largely unchanged [30], [31]. Under these circumstances, the SFL model owner cannot infer specific details about a client's data by observing the mechanism's output, thereby preserving privacy. From the study [14], introducing Gaussian noise to the smashed data degraded the quality of the reconstructed image, thereby enhancing privacy. If the SFL model owner permits clients to utilize DP during SFL training, the owner can potentially set a larger L_{\min} due to the reduced privacy concerns. In this context, we additionally perform the empirical study, shown in Table III. To examine the relationship between noise levels and privacy leakage, we utilized a training-based adversarial inversion approach. The CIFAR-10 dataset was used for training an SFL model, a shadow model, and a reconstruction model. The privacy risk was evaluated by measuring the perceptual similarity between original and reconstructed images using the Structural Similarity Index (SSIM). From this result, clients must carefully determine the noise level in DP, balancing the trade-off between privacy and accuracy. Moreover, when the client complexity is low ($L_c=3$ in this case), the accuracy of SFL is more sensitive to the added noise.

VII. CONCLUSION AND FUTURE WORK

This paper has studied the interaction between an SFL model owner and clients during the SFL process, formulated as a single-leader multi-follower Stackelberg game in competitive or conflict situations. Each client's strategy involves the amount of data contributed for local training, while the SFL model owner determines suitable incentives to motivate client participation in SFL. The SFL model owner also sets the cut layer to balance the training burden between clients and servers while trying to meet the required privacy level. Our results indicate that Stackelberg strategies are desirable operating points for all participants in competitive scenarios. For a more practical approach, future work may involve designing a more sophisticated incentive management game that considers unshared information between clients, detailed evaluations of client contributions, and computing and networking dynamics (such as a Stackelberg Bayesian game-based or deep reinforcement learning-based incentive management).

REFERENCES

- [1] J. Lee, F. Solat, T. Y. Kim, and H. V. Poor, "Federated Learning-Empowered Mobile Network Management for 5G and Beyond Networks: From Access to Core," *IEEE Communications Surveys & Tutorials*, vol. 26, no. 3, pp. 2176–2212, Jan. 2024.

- [2] C. Thapa, P. C. Mahawaga Arachchige, S. Camtepe, and L. Sun, "SplitFed: When Federated Learning Meets Split Learning," in *Proceedings of the 2022 Association for the Advancement of Artificial Intelligence (AAAI)*, 2022.
- [3] A. Singh, P. Vepakomma, O. Gupta, and R. Raskar, "Detailed Comparison of Communication Efficiency of Split Learning and Federated Learning," arXiv, 2019. [Online]. Available: <https://arxiv.org/abs/1909.09145>
- [4] H. Hafi, B. Brik, P. A. Frangoudis, A. Ksentini, and M. Bagaa, "Split Federated Learning for 6G Enabled-Networks: Requirements, Challenges and Future Directions," *IEEE Access*, vol. 12, pp. 9890–9930, Jan. 2024.
- [5] D.-J. Han, H. I. Bhatti, J. Lee, and J. Moon, "Accelerating Federated Learning with Split Learning on Locally Generated Losses," in *Proceedings of the 2021 International Conference on Machine Learning (ICML-Workshop of Federated Learning for User Privacy and Data Confidentiality)*, 2021.
- [6] W. Wu, M. Li, K. Qu, C. Zhou, X. Shen, W. Zhuang, X. Li, and W. Shi, "Split Learning Over Wireless Networks: Parallel Design and Resource Management," *IEEE Journal on Selected Areas in Communications*, vol. 41, no. 4, pp. 1051–1066, April 2023.
- [7] Y. Mu and C. Shen, "Communication and Storage Efficient Federated Split Learning," arXiv, 2023. [Online]. Available: <https://arxiv.org/abs/2302.05599v1>
- [8] Z. Lin, G. Zhu, Y. Deng, X. Chen, Y. Gao, K. Huang, and Y. Fang, "Efficient Parallel Split Learning over Resource-constrained Wireless Edge Networks," *IEEE Transactions on Mobile Computing*, pp. 1–16, to appear, 2024.
- [9] Y. Zhan, J. Zhang, Z. Hong, L. Wu, P. Li, and S. Guo, "A Survey of Incentive Mechanism Design for Federated Learning," *IEEE Transactions on Emerging Topics in Computing*, vol. 10, no. 2, pp. 1035–1044, 2022.
- [10] G. Zhu, Y. Deng, X. Chen, H. Zhang, Y. Fang, and T. F. Wong, "ESFL: Efficient Split Federated Learning over Resource-Constrained Heterogeneous Wireless Devices," *IEEE Internet of Things Journal*, vol. 11, no. 16, pp. 27 153–27 166, 2024.
- [11] F. Solat, J. Lee, and D. Nyato, "Split Federated Learning-Empowered Energy-Efficient Mobile Traffic Prediction Over UAVs," *IEEE Wireless Communications Letters*, vol. 13, no. 11, pp. 3064–3068, 2024.
- [12] J. Kim, S. Shin, Y. Yu, J. Lee, and K. Lee, "Multiple Classification with Split Learning," in *Proceedings of the 2020 International Conference on Smart Media and Applications (SMA)*, 2020.
- [13] P. Vepakomma, O. Gupta, A. Dubey, and R. Raskar, "Reducing Leakage in Distributed Deep Learning for Sensitive Health Data," in *Proceedings of the 2019 International Conference on Learning Representations (ICLR- AI for Social Good Workshop)*, 2019.
- [14] J. Lee, M. Seif, J. Cho, and H. V. Poor, "Exploring the Privacy-Energy Consumption Tradeoff for Split Federated Learning," *IEEE Network*, vol. 38, no. 6, pp. 388–395, May 2024.
- [15] —, "Optimizing Privacy and Latency Tradeoffs in Split Federated Learning over Wireless Networks," *IEEE Wireless Communications Letters*, pp. 1–1, to appear, 2024.
- [16] C. Huang, G. Tian, and M. Tang, "When MiniBatch SGD Meets SplitFed Learning: Convergence Analysis and Performance Evaluation," arXiv, 2023. [Online]. Available: <https://arxiv.org/abs/2308.11953>
- [17] H. Wang and J. Xie, "User Preference Based Energy-Aware Mobile AR System with Edge Computing," in *Proceedings of the 2020 IEEE Conference on Computer Communications (INFOCOM)*, 2020, pp. 1379–1388.
- [18] Q. Liu, S. Huang, J. Opadere, and T. Han, "An Edge Network Orchestrator for Mobile Augmented Reality," in *Proceedings of the 2018 IEEE Conference on Computer Communications (INFOCOM)*, 2018, pp. 756–764.
- [19] D. Niyato, M. A. Alsheikh, P. Wang, D. I. Kim, and Z. Han, "Market model and optimal pricing scheme of big data and Internet of Things," in *Proc. IEEE Int. Conf. Commun. (ICC)*, May 2016, pp. 1–6.
- [20] S. Luo, X. Chen, Q. Wu, Z. Zhou, and S. Yu, "HFEL: Joint Edge Association and Resource Allocation for Cost-Efficient Hierarchical Federated Edge Learning," *IEEE Transactions on Wireless Communications*, vol. 19, no. 10, pp. 6535–6548, 2020.
- [21] J. Kim, D. Kim, J. Lee, and J. Hwang, "A Novel Joint Dataset and Computation Management Scheme for Energy-Efficient Federated Learning in Mobile Edge Computing," *IEEE Wireless Communications Letters*, vol. 11, no. 5, pp. 898–902, 2022.
- [22] D. Doyeon, S. Shin, J. Jeong, and J. Lee, "Joint Edge Server Selection and Dataset Management for Federated Learning-Enabled Mobile Traffic Prediction," *IEEE Internet of Things Journal*, vol. 11, no. 3, pp. 4971–4986, Feb. 2024.
- [23] N. H. Tran, W. Bao, A. Zomaya, M. N. H. Nguyen, and C. S. Hong, "Federated Learning over Wireless Networks: Optimization Model Design and Analysis," in *Proceedings of the 2019 IEEE Conference on Computer Communications (INFOCOM)*, 2019, pp. 1387–1395.
- [24] T. Basar and G. J. Olsder, *Dynamic Noncooperative Game Theory*, 2nd. Philadelphia, PA, USA: SIAM, 1999.
- [25] M. J. Osborne and A. Rubinstein, *A Course in Game Theory*. Cambridge, Jun. 1994.
- [26] H. Roh, C. Jung, W. Lee, and D. Z. Du, "Resource Pricing Game in Geo-distributed Clouds," in *Proceedings of the 2013 IEEE Conference on Computer Communications (INFOCOM)*, 2013, pp. 1519–1527.
- [27] J. Lee, J. Guo, J. K. Choi, and M. Zukerman, "Distributed Energy Trading in Microgrids: A Game-Theoretic Model and Its Equilibrium Analysis," *IEEE Transactions on Industrial Electronics*, vol. 62, no. 6, pp. 3524–3533, Jun. 2015.
- [28] A. Krizhevsky, G. Hinton *et al.*, "Learning Multiple Layers of Features from Tiny Images," Master's thesis, University of Toronto, 2009.
- [29] H. Xiao, K. Rasul, and R. Vollgraf, "Fashion-MNIST: a Novel Image Dataset for Benchmarking Machine Learning Algorithms," arXiv, 2017.
- [30] S. Kalra, J. Wen, J. C. Cresswell, M. Volkovs, and H. R. Tizhoosh, "Decentralized Federated Learning Through Proxy Model Sharing," *Nature Communications*, vol. 14, no. 2899, May 2023.
- [31] C. Dwork, A. Roth *et al.*, "The Algorithmic Foundations of Differential Privacy," *Foundations and Trends® in Theoretical Computer Science*, vol. 9, no. 3–4, pp. 211–407, 2014.